Passive simulation of electrodynamic loudspeakers for guitar amplifiers: a port- Hamiltonian approach

Antoine Falaize, Thomas Hélie

Passive simulation of electrodynamic loudspeakers for guitar amplifiers: a port- Hamiltonian approach

A. Falaize and T. Hélie
IRCAM, 1 place Igor Stravinsky, 75004 Paris, France
antoine.falaize@ircam.fr

Because of technological constraints, transducers are usually not ideal. In musical and audio applications, this is the case of electrodynamic loudspeakers used eg. in guitar amplifiers. Thus, to build realistic numerical simulations of such systems, it is important to pay close attention to their non ideality. These systems include several nonlinearities, mainly due to mechanical suspensions, magnetic properties and temperature variations. At the same time, it is not straightforward to model such refinements while preserving basic physical properties such as causality, stability, passivity. In this paper, we introduce a new modeling of loudspeaker which includes fractional order dynamics and nonlinearities, such that the power balance is guaranteed. Since the mechanical-acoustic coupling is well described in the literature, we focus on the functioning of loudspeaker in the electrical, magnetical and mechanical domains, applying a standard acoustical load on the diaphragm. The approach is based on *Port-Hamiltonian Systems* theory. This formalism naturally preserves the energetic behavior of elementary components and the power balance, including the nonlinear case. In conjunction, we describe the nonlinearities due to the lossy coil in terms of fractional derivative. This permit to well approximate the nonlinear electrical impedance using a reduced number of parameters, still preserving passivity of continuous-time models despite the approximation. By transcribing this property in the digital domain, we guarantee the stability of the simulations. Thermodynamic effects are neglected in this preliminary work, but can directly be incorporated in the Port-Hamiltonian model.

Introduction

For several acoustic instruments (such as guitars, keyboards, strings, etc.), an electric version exists. These electric instruments require amplification. This stage of the audio chain has a determinant influence on the audio output. *Combo amplifiers*, which include conditioning, processing, amplification, and finally transduction are generally used. These complex nonlinear systems integrate several physical fields: electrical, magnetic, mechanical, acoustic, and also thermal effects (see *eg.* [1, 2]). Thus, building a realistic digital simulation of *electric input* to *acoustical output* behavior of these systems is a challenge. In a divide and conquer strategy, we focus here on the transducer, namely the electrodynamic loudspeaker. Those systems are well-known electrodynamic systems whose use has been widespread, whether in sound diffusion or as a part of measurement systems (musical and room acoustic, nondestructive testing, etc.). However, they are themselves complex nonlinear systems coupling between multiple physical domains. For these reasons, it is difficult to predict their response to varied stimuli.

An electrodynamic loudspeaker is classically described by the Thiele and Small model [3, 4], which is valid when the system is used in its linear operating region. However, this model does not reflect all the nuances that appear when the system is used at high level. The modeling of non-linear effects have been extensively studied and several methods have been proposed: variation of the Thiele and Small parameters [5, 6], Volterra [7] and Wiener-Volterra [8] series, or nonlinear state representation [9, 10]. However, the physical interpretation of these various models and the preservation of passivity is not obvious. Moreover, the moving coil has a solid iron core, inducing fractional order dynamic [11, 12].

In this paper, we propose a simplified model of the electrodynamic loudspeaker, preserving the inherent passivity of the original physical system. This model is given in the formalism of " Port-Hamiltonian Systems". It includes in particular fractional order dynamic for the coil and nonlinear stiffness for the suspension. Thermal effects are neglected, and acoustic load is expressed as an external source of power.

The paper is organized as follows. The Port-Hamiltonian framework is recalled section 1. In section 2 we recast the lossy coil as a fractional order integrator and give its port-Hamiltonian formulation. Section 3 is devoted to the formulation of the complete model, including the non-linear stiffness. Finally, a first order numerical scheme preserving passivity and simulation results are given section 4.

1 Port-Hamiltonian Systems: basics and introductory example

We firstly present the PHS framework. Note that our formulation of SHP is slightly different from that found in the literature [13, 14, 15] since the memoryless (*ie.* dissipative) part of the system is computed aside, introducing a dissipative state. Then we give an illustrative example.

1.1 Formalism

Physical systems proves passive. They are made of:

- storage components with total energy $\mathtt{E}(t) \geq 0$
- dissipative components with dissipated power $P_{\mathcal{D}}(t) \geq 0$
- external ports with total provided power $P_{\mathcal{S}}(t)$.

Port Hamiltonian Systems (PHS) encode this passivity property through the power balance

$$\frac{\mathrm{d}\mathtt{E}(t)}{\mathrm{d}t} = -P_{\mathcal{D}}(t) + P_{\mathcal{S}}(t). \tag{1}$$

The *Hamiltonian* is the total energy $\mathcal{H} : \mathbf{x} \mapsto \mathcal{H}(\mathbf{x}) \in \mathbb{R}_+$ expressed on a choosen *state* $\mathbf{x} \in \mathbb{R}^{n_S}$ so that $\frac{\mathrm{d}\mathtt{E}}{\mathrm{d}t} = \nabla\mathcal{H}(\mathbf{x})^T \frac{\mathrm{d}\mathbf{x}}{\mathrm{d}t}$. The dissipated power is factorized as $P_{\mathcal{D}} = \mathbf{z}(\mathbf{w})^T\mathbf{w}$ with $\mathbf{w} \in \mathbb{R}^{n_D}$ a choosen *dissipative state* and $\mathbf{z} : \mathbb{R}^{n_D} \to \mathbb{R}^{n_D}$ a *dissipation function*. A similar factorization is done for external sources with *input* vector $\mathbf{u} \in \mathbb{R}^{n_P}$ and *output* vector $\mathbf{y} \in \mathbb{R}^{n_P}$ so that $P_{\mathcal{S}} = \mathbf{u}^T\mathbf{y}$. A *port-Hamiltonian system* is the structure (2), with $\mathbf{J}_\mathbf{x} \in \mathbb{R}^{n_S \times n_S}$, $\mathbf{J}_\mathbf{w} \in \mathbb{R}^{n_D \times n_D}$, $\mathbf{J}_\mathbf{y} \in \mathbb{R}^{n_P \times n_P}$ skew symmetric matrices (such that $\mathbf{J}^T = -\mathbf{J}$). This structure restores the power balance since $\mathbf{S}$ is skew-symmetric: $B^T A = B^T \mathbf{S} B = \frac{\mathrm{d}\mathtt{E}}{\mathrm{d}t} + P_{\mathcal{D}} - P_{\mathcal{S}} = 0$.

$$\underbrace{\left(\begin{array}{c} \frac{\mathrm{d}\mathbf{x}}{\mathrm{d}t} \\ \hline \mathbf{w} \\ \hline -\mathbf{y} \end{array}\right)}_{A} = \underbrace{\left(\begin{array}{c|c|c} \mathbf{J}_\mathbf{x} & -\mathbf{K} & \mathbf{G}_\mathbf{x} \\ \hline \mathbf{K}^T & \mathbf{J}_\mathbf{w} & \mathbf{G}_\mathbf{w} \\ \hline -\mathbf{G}_\mathbf{x}{}^T & -\mathbf{G}_\mathbf{w}{}^T & \mathbf{J}_\mathbf{y} \end{array}\right)}_{\mathbf{S}} \cdot \underbrace{\left(\begin{array}{c} \nabla\mathcal{H}(\mathbf{x}) \\ \hline \mathbf{z}(\mathbf{w}) \\ \hline \mathbf{u} \end{array}\right)}_{B} \tag{2}$$

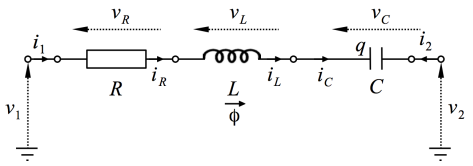

Figure 1: A simple RLC circuit.

1.2 Example

Consider the simple *RLC*-circuit of figure 1, where q is the charge on one of the two plates of the capacitor with capacitance C and ϕ is the magnetic flux considered in the solenoid with inductance L. R is a linear resistor. The two storage components are the capacitor C and the inductor L with energies $\mathcal{H}_C(q) = q^2/(2C)$ and $\mathcal{H}_L(\phi) = \phi^2/(2L)$ respectively. The Hamiltonian is $\mathcal{H}(\mathbf{x}) = \mathcal{H}_C(x_1) + \mathcal{H}_L(x_2)$, with the state $\mathbf{x} = (q, \phi)^T$, so that $\nabla\mathcal{H}(\mathbf{x}) = (e_C, i_L)^T$ and $\frac{\mathrm{d}\mathbf{x}}{\mathrm{d}t} = (i_C, e_L)^T$. The power dissipated in the resitor is $P_{\mathcal{D}} = z(w)w$ with the state $w = i_R$ and the linear characteristic $z(w) = Rw = e_R$. The input is $\mathbf{u} = (e_1, e_2)^T$ and the output is $\mathbf{y} = (i_1, i_2)^T$. Applying Kirchhoff's laws, the dynamic of this circuit is recasted as the PHS (2), with

$$\mathbf{J_x} = \begin{pmatrix} 0 & +1 \\ -1 & 0 \end{pmatrix}, \quad \mathbf{K} = \begin{pmatrix} 0 \\ +1 \end{pmatrix}, \quad \mathbf{G_x} = \begin{pmatrix} 0 & 0 \\ +1 & -1 \end{pmatrix},$$
$$\mathbf{J_w} = 0, \quad \mathbf{G_w} = (0, 0), \quad \mathbf{J_y} = \begin{pmatrix} 0 & 0 \\ 0 & 0 \end{pmatrix}.$$

Note that replacing linear components by nonlinear ones lets the structure matrices unchanged. A method to automatically generate this structure for analog circuit based on a dictionary of elementary components and graph theory is described in [16]. The next section is devoted to the PHS formulation of the fractional moving coil.

2 Fractional moving coil

The standard linear inductor of example 1.2 can be expressed as a PHS with state $x_L = \phi$, input $u_L = e_L = \frac{\mathrm{d}x_L}{\mathrm{d}t}$ and output $y_L = i_L = \frac{\mathrm{d}\mathcal{H}_L}{\mathrm{d}\phi}$:

$$\begin{pmatrix} \frac{\mathrm{d}x_L}{\mathrm{d}t} \\ -y_L \end{pmatrix} = \begin{pmatrix} 0 & 1 \\ -1 & 0 \end{pmatrix} \cdot \begin{pmatrix} \frac{\partial\mathcal{H}_L(x_L)}{\partial x_L} \\ u_L \end{pmatrix}, \tag{3}$$

so the energy stored in a storage component is obtained by accumulation of the input through the storage function $\mathcal{H}_L(x_L) = \mathcal{H}_L\left(\int_0^t u(\tau)\mathrm{d}\tau\right)$. Thus the fractional coil has to be considered as a fractional integrator [11, 12]. In Laplace domain:

$$i_\alpha(s) = \frac{e_\alpha(s)}{L_\alpha s^\alpha} \tag{4}$$

where s is the complex frequency and L_α is of unit $[\mathrm{V}].[\mathrm{T}]^\alpha.[\mathrm{A}]^{-1}$. First, we recast the fractional integrator as an infinite dimensional PHS. Second, we give the finite dimensional approximation for practical implementation.

2.1 PHS formulation of fractional integrator

Here we build a PHS which restores the fractional integrator of order $\alpha \in]0, 1[$. A well established formalism for the realization of such transfer functions exists: the so called *diffusive representation* [17]. The complete theory is out the scope of this paper, but we recall the main steps of the method. Defining $s = \rho.e^{i\theta}$, with $\rho \geq 0$ and $\theta \in [-\pi, \pi[$, the transfer function of the fractional integrator $T_\alpha(s) = s^{-\alpha}$ exhibits a cut $C = \mathbb{R}_-$. The jump of T_α across C is $\mu(-\xi \in C)$:

$$\mu(-\xi) = \frac{T_\alpha(-\xi - i0^+) - T_\alpha(-\xi + i0^+)}{2i\pi} = \frac{sin(\beta\pi)}{\pi\xi^\alpha}. \tag{5}$$

The residue theorem gives a realization of the transfer function as the sum of contributions of the singularities along the cut (weighted continuous aggregation of linear damping $T_\xi(s) = \frac{1}{s+\xi}$, $\xi \in \mathbb{R}^+$):

$$T_\alpha(s) = \int_0^{+\infty} \frac{\mu(-\xi)\cdot\mathrm{d}\xi}{1+\xi}, \tag{6}$$

which is well posed since $\int_0^{+\infty} \left|\frac{\mu(-\xi)\cdot\mathrm{d}\xi}{1+\xi}\right| < \infty$. Defining the output of the fractional integrator as $y_\alpha(s) = T_\alpha(s).u_\alpha(s)$, an *input - state - output* representation is:

$$\begin{cases} \frac{\mathrm{d}x_\xi}{\mathrm{d}t} & = -\xi \cdot x_\xi + u_\alpha, \quad x_\xi(0) = 0, \\ y_\alpha & = \int_0^{+\infty} \mu(-\xi) \cdot x_\xi \cdot \mathrm{d}\xi. \end{cases} \tag{7}$$

The system (7) can be written as a PHS with *inductance density* $L_\xi = \frac{1}{\mu(-\xi)}$, *hamiltonian density* $\mathcal{H}_\xi(x_\xi) = x_\xi^2/(2L_\xi)$ and *resistance density* $R_\xi = L_\xi \cdot \xi$. The total energy is $\mathcal{H}_\alpha(\mathbf{x}_\alpha) = \int_{\xi\in C} \mathcal{H}_\xi(x_\xi)\mathrm{d}\xi$ with infinite dimensional state $\mathbf{x}_\alpha \in \mathbb{R}^{\mathbb{R}_+}$. We denote the concatenation of local Hamiltonian gradient $\frac{\mathrm{d}\mathcal{H}_\xi}{\mathrm{d}x_\xi}$ and local dissipation $z_\xi(w_\xi) = R_\xi.w_\xi$ for all $\xi \in C$ by $\nabla\mathcal{H}_\alpha(\mathbf{x}_\alpha)$ and $\mathbf{z}(\mathbf{w}_\alpha)$ with $\mathbf{w}_\alpha \in \mathbb{R}^{\mathbb{R}_+}$ respectively. Then the PHS corresponding to (7) is

$$\left(\begin{array}{c} \frac{\mathrm{d}\mathbf{x}_\alpha}{\mathrm{d}t} \\ \hline \mathbf{w}_\alpha \\ \hline y_\alpha \end{array}\right) = \left(\begin{array}{c|c|c} \mathbb{0}_{\infty\times\infty} & -\mathbb{I}_\infty & \mathbb{1}_{\infty\times 1} \\ \hline \mathbb{I}_\infty & \mathbb{0}_{\infty\times\infty} & \mathbb{0}_{\infty\times 1} \\ \hline \mathbb{1}_{1\times\infty} & \mathbb{0}_{1\times\infty} & \mathbb{0}_{1\times 1} \end{array}\right) \cdot \left(\begin{array}{c} \nabla\mathcal{H}_\alpha(\mathbf{x}_\alpha) \\ \hline \mathbf{z}_\alpha(\mathbf{w}_\alpha) \\ \hline u_\alpha \end{array}\right), \tag{8}$$

with $\mathbb{0}$ a matrix full of 0, $\mathbb{1}$ a matrix full of 1, and $\mathbb{I}$ the identity matrix, each with proper dimensions. The realization of the coil (4) with transfert function $T_{L_\alpha}(s) = (L_\alpha \cdot s^\alpha)^{-1}$ is given by system (8), with $L_\xi = \frac{L_\alpha}{\mu(-\xi)}$.

2.2 Finite order approximation

For implementation, finite approximation of diffusive representation (6) is built based on a finite set of poles $-\xi_n$ localized on the cut C. Here we strictly apply the method given in [17, sec. 5.1.2] to obtain a least square optimization of the weights $\boldsymbol{\mu} = (\mu_1 \cdots \mu_N)^T$ by minimizing an appropriate distance between T_α and its discretisation $\widehat{T}_\alpha$.

$$\widehat{T}_\alpha(s) \sum_{n=1}^{N} \frac{\mu_n}{s+\xi_n} = \mathbf{E}(s) \cdot \boldsymbol{\mu}; \quad \mathbf{E}(s) = \left(\begin{array}{ccc} \frac{1}{s+\xi_1} & \cdots & \frac{1}{s+\xi_N} \end{array}\right)^T \tag{9}$$

with $\mathbf{E}(s) = \left(\frac{1}{s+\xi_1} \cdots \frac{1}{s+\xi_N}\right)^T$. To obtain an accurate approximations on the audible range ($F^- = 20\,\mathrm{Hz}$ to $F^+ = 20\,\mathrm{kHz}$), function $\omega \mapsto G_\alpha(s = i\omega)$ must be accurately approximated on the (dimensionless) angular frequency range $\omega_{min} = \frac{F^-}{F_c^+} = 10^{-3}$ to $\omega_{max} = \frac{F^+}{F_c^-} = 10^{+3}$. Additionally, frequencies are perceived according to a logarithmic scale, so the poles ξ_n's are chosen as

$$-\xi_n = -1 - 10^{\ell_n} \in C, \text{ for } 0 \leq n \leq N+1, \tag{10}$$

where the ℓ_n's are equally spaced, with step $\delta = \frac{\ell_{N+1}-\ell_0}{N+1}$, from ℓ_0 to ℓ_{N+1} . Finally, gain deviations are perceived relatively to the reference gains, so the weights μ, are optimized with respect to the objective function

$$O(\boldsymbol{\mu}) = \int_{\omega_{min}}^{\omega_{max}} \left| 1 - \frac{\widehat{T}_\alpha(s=i\omega)}{T_\alpha(s=i\omega)} \right|^2 \mathrm{d}\ln\omega. \tag{11}$$

In practice, the integral in (11) is approximated by a finite sum on a frequency grid, here, $\ln\omega_k = \ln\omega_{min} + \frac{k}{K}\ln\frac{\omega_{max}}{\omega_{min}}$ for $0 \leq k \leq K$. Moreover, a regularization term (standard Tikhonov penalty proportional to $\boldsymbol{\mu}^T\boldsymbol{\mu}$) is required to avoid ill-conditioned matrix inversion if $N = \dim(\boldsymbol{\mu})$ is not sufficiently small. This yields the following practical objective function

$$\widehat{O}(\mu) = \overline{(\mathbf{M}\boldsymbol{\mu} - \mathbf{T})}^T \mathbf{W}(\mathbf{M}\boldsymbol{\mu} - \mathbf{T}) + \varepsilon\boldsymbol{\mu}^T\boldsymbol{\mu}, \tag{12}$$

where $\omega_{k-\frac{1}{2}} = \sqrt{\omega_{k-1}\omega_k}$ denotes the geometric mean of ω_{k-1} and ω_k for $1 \leq k \leq K$. Matrix $\mathbf{M}$ is composed of the rows $[\mathbf{M}]_{k,*} = \mathbf{E}(s = i\omega_{k-\frac{1}{2}})^T$ defined in (9), vector $\mathbf{T}$ is composed of $[\mathbf{T}]_k = T_\alpha(s = i\omega_{k-\frac{1}{2}})$ and the diagonal matrix $\mathbf{W}$ is defined by $[\mathbf{W}]_{k,k} = (\ln\omega_k - \ln\omega_{k-1}) \,/\, \left|[\mathbf{T}]_k\right|^2$. The Tikhonov penalty parameter $\varepsilon \geq 0$ is automatically adjusted by dichotomy and testing the condition number, in order that the final condition number of the inverse matrix is larger than the float precision. The minimization of (12) is straightforward: first, the complex values in $\mathbf{M}$ and $\mathbf{T}$ are decomposed into their real and imaginary parts; second, this standard least square problem is analytically solved; third, the analytic result is recomposed into a closed form with respect to the complex quantities for conciseness. This yields the real-valued optimal weights

$$\boldsymbol{\mu}^{opt} = \left(\overline{\mathbf{M}}^T\mathbf{W}\mathbf{M} + \epsilon\mathbb{I}_N\right)^{-1} \cdot \mathcal{R}e\left(\overline{\mathbf{M}}^T\mathbf{W}\mathbf{T}\right). \tag{13}$$

Defining $L_n = \frac{L_\alpha}{\mu_n^{opt}}$ and $R_n = L_n \cdot \xi_n$ for all $n \in [1 \cdots N]$, the finite dimensional PHS for the realization of the lossy coil is composed of N inductors with energies $\mathcal{H}_n(x_n) = \frac{x_n^2}{2L_n}$ and N resistors with dissipations $z_n(w_n) = R_n \cdot w_n$. It reads as

$$\left(\begin{array}{c} \frac{\mathrm{d}\hat{\mathbf{x}}_\alpha}{\mathrm{d}t} \\ \hat{\mathbf{w}}_\alpha \\ \hline \hat{y}_\alpha \end{array}\right) = \left(\begin{array}{c|c|c} \mathbb{O}_{N\times N} & -\mathbb{I}_N & \mathbb{1}_{N\times 1} \\ \hline \mathbb{I}_N & \mathbb{O}_{N\times N} & \mathbb{O}_{N\times 1} \\ \hline \mathbb{1}_{1\times N} & \mathbb{O}_{1\times N} & \mathbb{O}_{1\times 1} \end{array}\right) \cdot \left(\begin{array}{c} \nabla\widehat{\mathcal{H}}_\alpha(\hat{\mathbf{x}}_\alpha) \\ \hat{\mathbf{z}}_\alpha(\hat{\mathbf{w}}_\alpha) \\ \hline \hat{u}_\alpha \end{array}\right), \tag{14}$$

choosing the states $\hat{\mathbf{x}}_\alpha = (x_1 \cdots x_N)^T$ and $\hat{\mathbf{w}}_\alpha = (w_1 \cdots w_N)^T$, the total energy being $\widehat{\mathcal{H}}_\alpha(\hat{\mathbf{x}}_\alpha) = \sum_{n=1}^N \frac{x_n^2}{2L_n}$ and the total dissipation function being $\hat{\mathbf{z}}_\alpha(\hat{\mathbf{w}}_\alpha) = (z_1(w_1)\cdots z_N(w_N))^T$. This correspond to the parallel connection of N serial RL components (see figure 2). This model is used in the next section to build the PHS of the electrodynamic loudspeaker.

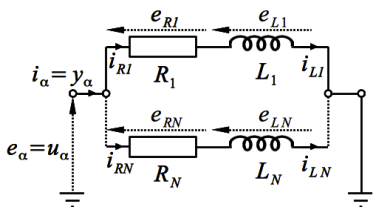

Figure 2: Element realizing the fractional lossy coil.

3 PHS model of the loudspeaker

Firstly we recast a linear model of the loudspeaker in PHS formalism using well known electro-mechanical analogy. Secondly we built a parametric nonlinearity to model the stiffness due to the surround and the spider. Thirdly we design a numerical scheme that preserves passivity for solving the system's dynamic. Finally, simulation results for a "" are given.

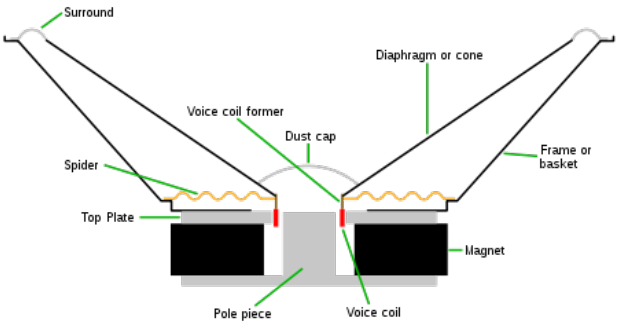

Figure 3: Sectional view of a loudspeaker.

3.1 Port-Hamiltonian formulation of the standard model

A well established electronic analog of the loudspeaker is given figure 6. Choosing the momentum as the state of the mass $x_m = m.v_m$, the kinetic energy is $\mathcal{H}_m(x_m) = \frac{x_m^2}{2.m}$. Newton's law of dynamic is then $\frac{\mathrm{d}x_m}{\mathrm{d}t} = F_m$, and $\frac{\mathrm{d}\mathcal{H}_m(x_m)}{\mathrm{d}x_m} = v_m$. With the analogies (see *eg.* [3, 4]) $i \leftrightarrow v$ and $e \leftrightarrow F$, the mass is equivalent to an inductance with $L = m$. Similarly, choosing the deviation from the equilibrium as the state for the linear stiffness K, the potential energy is $\mathcal{H}_K(x_K) = K\frac{x_K^2}{2}$. Using the previous analogies, it corresponds to a capacitance with $C = \frac{1}{K}$. Choosing $w_a = v_m$, the damping function is $F_a = z_a(w_a) = R_a.w_a$, which corresponds to a resistance.

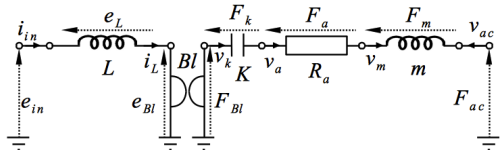

Figure 4: Basic electric analog of the loudspeaker.

The acoustical port variables are the fluid velocity v_{ac} which is supposed to *stick* at the diaphragm, and the force F_{ac} due to the gradient of pressure between the two sides of the diaphragm. The electro-mechanical conversion (*ie.* Laplace force) is modeled as a conservative gyrator with ratio Bl: $F_{Bl} = Bl.i_L$ and $e_{Bl} = Bl.v_m$. Finally, the loudspeaker can be recasted as the PHS (15).

$$\left(\begin{array}{c} e_L \\ F_m \\ v_k \\ \hline v_a \\ \hline -i_{in} \\ -v_{ac} \end{array}\right) = \left(\begin{array}{ccc|ccc} 0 & -Bl & 0 & 0 & -1 & 0 \\ +Bl & 0 & -1 & -1 & 0 & +1 \\ 0 & +1 & 0 & 0 & 0 & 0 \\ \hline 0 & +1 & 0 & 0 & 0 & 0 \\ \hline +1 & 0 & 0 & 0 & 0 & 0 \\ 0 & -1 & 0 & 0 & 0 & 0 \end{array}\right) \left(\begin{array}{c} i_L \\ v_m \\ F_k \\ \hline F_a \\ \hline e_{in} \\ F_{ac} \end{array}\right) \tag{15}$$

3.2 Non-linear stiffness

The main non-linearity is the saturation effect of the spider's stiffness (see *eg.* [5, 6]). In this section, we built a parametric storage function which phenomenologically restores the saturation, preserving passivity. Here, $\nabla\mathcal{H}_K(x)$ is a linear combination of odd basis functions so that the main part of the system is linear with respect to parameters $(K_0,\ K_{sat})$:

$$\nabla\mathcal{H}_K(x) = K_0 c_0(x) + K_{sat} c_{sat}\left(\frac{x}{x_{sat}}\right) \tag{16}$$

with $c_0(x)$ the linear behaviors around origin and $c_{sat}(x)$ the saturation normalized in $x = \frac{x_{sat}}{2}$. We choose $c_0(x) = x$ and $c_{sat}(x) = \frac{4}{4-\pi}.\left(\tan(\frac{\pi.x}{2}) - \frac{\pi.x}{2}\right)$. The associated energy is

$$\tilde{\mathcal{H}}_K(x) = \int_0^x c(\tilde{x})d\tilde{x} = K_0.\mathcal{H}_0(x) + K_{sat}.\mathcal{H}_{sat}\left(\frac{x}{x_{sat}}\right) \tag{17}$$

with $\mathcal{H}_{sat}(x) = -\frac{8.x_{sat}}{\pi(4-\pi)}.\left(\ln\left|\cos\left(\frac{\pi.x}{2}\right)\right| + \frac{\pi^2}{8}.x^2\right)$ and $\mathcal{H}_0(x) = \frac{x^2}{2}$. Then $\mathcal{H}_K(x) \geq 0$ for all $(K_0, K_{sat}) \in \mathbb{R}_*^+ \times \mathbb{R}_*^+$.

3.3 Final model

Simply replacing the linear stiffness by the non-linear version from section 3.2 and the standard inductance by the fractional version (14) in (15), the proposed PHS model of the electrodynamic loudspeaker is

$$\left(\begin{array}{c}\frac{\delta\mathbf{x}_l}{2\delta T}\\ \frac{\delta x_K}{2\delta T}\\ \hline \mathbf{w}\\ \hline -\mathbf{y}\end{array}\right) = \left(\begin{array}{c|c|c|c} \mathbf{J}_l & \mathbf{J}_{lnl} & -\mathbf{K}_l & \mathbf{G}_l\\ \hline -\mathbf{J}_{lnl}{}^T & . & . & .\\ \hline \mathbf{K}_l{}^T & . & . & .\\ \hline -\mathbf{G}_l{}^T & . & . & .\end{array}\right)\cdot\left(\begin{array}{c}\delta_{\mathbf{x}}\bar{\mathcal{H}}(\bar{\mathbf{x}},\delta\bar{\mathbf{x}})\\ \hline \delta_x\tilde{\mathcal{H}}_K(\tilde{x}_K,\delta\tilde{x}_K)\\ \hline \mathbf{z}(\mathbf{w})\\ \hline \mathbf{u}\end{array}\right) \tag{18}$$

with

$$\begin{aligned}
\mathbf{x} &= (\hat{x}_1\cdots\hat{x}_N, x_m, \tilde{x}_K)^T,\\
\nabla\mathcal{H}(\mathbf{x}) &= (\partial_x\widehat{\mathcal{H}}_1(x_1)\cdots\partial_x\widehat{\mathcal{H}}_N(x_N), \partial_x\mathcal{H}_m(x_m), \partial_x\tilde{\mathcal{H}}_K(\tilde{x}_K))^T,\\
\mathbf{w} &= (\hat{w}_1\cdots\hat{w}_N, w_R, w_a)^T,\\
\mathbf{z}(\mathbf{w}) &= (\hat{z}_1(\hat{w}_1),\cdots,\hat{z}_N(\hat{w}_N), z_R(w_R), z_a(w_a))^T,\\
\mathbf{u} &= (e_{in}, F_{ac})^T,\\
\mathbf{y} &= (i_{in}, v_{ac})^T.
\end{aligned}$$

$$\mathbf{J}_l = \begin{pmatrix}\mathbb{0}_{N,N} & -Bl\cdot\mathbb{1}_{N,1}\\ +Bl\cdot\mathbb{1}_{1,N} & 0\end{pmatrix},\ \mathbf{J}_{lnl} = \begin{pmatrix}\mathbb{0}_{N,1}\\ -1\end{pmatrix}$$

$$\mathbf{K}_l = \begin{pmatrix}\mathbb{I}_N & \mathbb{0}_{N,1}\\ \mathbb{0}_{1,N} & -1\end{pmatrix};\ \mathbf{G}_l = \begin{pmatrix}+\mathbb{1}_{N,1} & \mathbb{0}_{N,1}\\ 0 & -1\end{pmatrix}$$

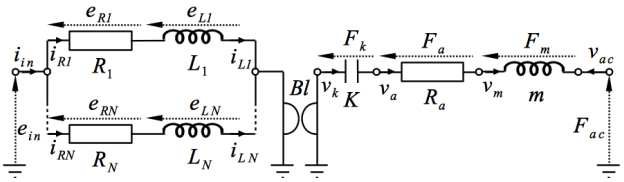

Figure 5: ?

4 Numerical simulation and results

In this section, a numerical scheme is specially designed so that a numerical time version of the power balance (1) is satisfied.

4.1 Discrete-time version of the power balance

Applying the midpoint rule $\delta_t\mathtt{E}(k) = \frac{\mathtt{E}(k+1)-\mathtt{E}(k-1)}{2\delta T}$, with k the sample number and δT the sampling period, a numerical approximation of (1) is $\delta_t\mathtt{E}(k) = P_{\mathcal{S}}(k) - P_{\mathcal{D}}(k)$. $\mathtt{E} = \mathcal{H}(\mathbf{x})$ is a composed function of time. This leads to introduce the discrete hamiltonian gradient so that

$$\left[\delta_{\mathbf{x}}\mathcal{H}(\mathbf{x},\delta\mathbf{x})\right]_s = \frac{\mathcal{H}_s[x_s(k)+\frac{1}{2}\delta x_s(k)] - \mathcal{H}_s[x_s(k)-\frac{1}{2}\delta x_s(k)]}{\delta x_s(k)}, \tag{19}$$

where $\delta x_s(k) = x_s(k+1) - x_s(k-1),\ \forall s \in [1\cdots n_S]$. Note that for a set of nl linear storage components $h_s(x_s) \equiv \frac{x_s^2}{2C_s}$, $\delta_{\mathbf{x}_l}\mathcal{H}_l(\mathbf{x}_l) = \mathbf{Q}\mathbf{x}_l$ with $\mathbf{Q} = \mathrm{diag}(x_1\cdots x_{n_l})$ and $\mathcal{H}_l = \sum_{s=1}^{n_l} h_s$. Specially designed numerical scheme preserving the stability for solving equation (1) is given by:

$$\delta_t\mathtt{E}(k) \quad = \quad \left[\delta_{\mathbf{x}}\mathcal{H}(\mathbf{x},\delta\mathbf{x})\right]^T.\delta_t\mathbf{x}(k)$$

where $\delta_t\mathbf{x}(k) = \frac{\mathbf{x}(k+1)-\mathbf{x}(k-1)}{2\delta T}$. Hence, a numerical version of system (2) preserving the passivity is given by

$$\left(\begin{array}{c}\frac{\delta\mathbf{x}_l}{2\delta T}\\ \frac{\delta x_K}{2\delta T}\\ \hline -\mathbf{y}\end{array}\right) = \left(\begin{array}{c|c|c} \mathbf{J}_l - \mathbf{K}_l\mathbf{R}\mathbf{K}_l{}^T & \mathbf{J}_{lnl} & \mathbf{G}_l\\ \hline -\mathbf{J}_{lnl}{}^T & . & .\\ \hline -\mathbf{G}_l{}^T & . & .\end{array}\right)\cdot\left(\begin{array}{c}\mathbf{Q}\mathbf{x}_l\\ \hline \delta_x\tilde{\mathcal{H}}_K(\tilde{x}_K,\delta\tilde{x}_K)\\ \hline \mathbf{u}\end{array}\right) \tag{20}$$

$$\delta_{\mathbf{x}}\bar{\mathcal{H}}(\bar{\mathbf{x}},\delta\bar{\mathbf{x}}) = \tfrac{1}{2}\mathbf{Q}(2\bar{\mathbf{x}}(n) + \delta\bar{\mathbf{x}}(n))$$

4.2 Simulation algorithm

Denoting by $\mathcal{T}$ the number of time-steps, the simulation procedure is given in algorithm 1.

$\mathbf{x}_l(1) \leftarrow \mathbb{0}$
$\tilde{x}_K(1) \leftarrow 0$
for $n = 1$ *to* $\mathcal{T}$ **do**
  $\mathtt{dxHl} \leftarrow \mathbf{Q}.\mathbf{x}_l(n)$
  $\delta\tilde{x}_K(n) \leftarrow -2.\delta T.\mathbf{J}_{lnl}{}^T.\mathtt{dxHl}$
  $\mathtt{dxHk} \leftarrow \delta_x\tilde{\mathcal{H}}_K(\tilde{x}_K(n), \delta\tilde{x}_K(n))$
  $\delta\mathbf{x}_l(n) \leftarrow 2.\delta T.[(\mathbf{J}_l - \mathbf{K}_l\mathbf{R}\mathbf{K}_l{}^T).\mathtt{dxHl} + \mathbf{J}_{lnl}.\mathtt{dxHk} + \mathbf{G}_l.u(n)]$
  $\mathbf{x}_l(n+1) \leftarrow \mathbf{x}_l(n) + \frac{1}{2}\delta\mathbf{x}_l(n)$
  $\tilde{x}_K(n+1) \leftarrow \tilde{x}_K(n) + \frac{1}{2}\delta\tilde{x}_K(n)$
  $\mathbf{w}(n) \leftarrow \mathbf{K}_l{}^T.\mathtt{dxHl}$
  $\mathbf{y}(n) \leftarrow \mathbf{G}_l{}^T.\mathtt{dxHl}$

Algorithm 1: Simulation algorithm

5 Conclusion

Thank you for your efforts in following these instructions, and welcome to the Acoustics 2012 Nantes conference!

Acknowledgments

The acknowledgment section should not be numbered (MS Word users should apply the **Reference heading** style) and should be located before the reference section.

References

[1] Darr, J. (1966). Electric guitar amplifier handbook. W. Foulsham.

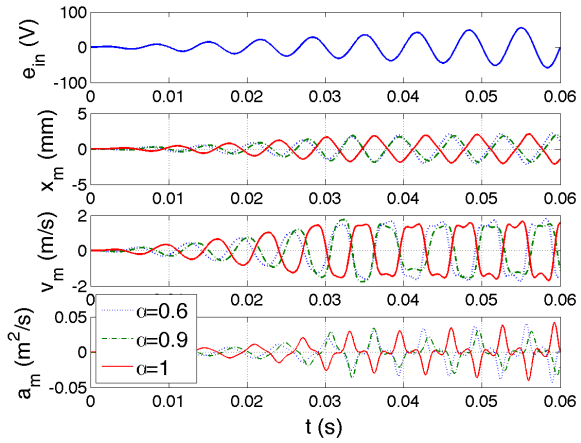

Figure 6: Simulation results.

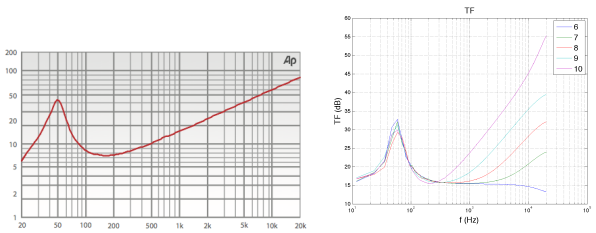

(a) Manufacturer (b) Simulated

Figure 7: Input electrical impedance, provided by the manufacturer in 7(a) and simulated in 7(b) for several orders of derivative $\alpha \in [0.6, 1]$.

[2] de Paiva, R. C. D., Pakarinen, J., Välimäki, V., & Tikander, M. (2011). Real-time audio transformer emulation for virtual tube amplifiers. EURASIP Journal on Advances in Signal Processing, 2011(1), 347645.

[3] Thiele, N. (1971). Loudspeakers in vented boxes: Part 1. Journal of the Audio Engineering Society, 19(5), 382-392.

[4] Thiele, N. (1971). Loudspeakers in vented boxes: Part 2. Journal of the Audio Engineering Society, 19(6), 471-483.

[5] Klippel, W. (1990). Dynamic measurement and interpretation of the nonlinear parameters of electrodynamic loudspeakers. Journal of the Audio Engineering Society, 38(12), 944-955.

[6] Klippel, W. (2005, October). Loudspeaker Nonlinearities - Causes, Parameters, Symptoms. In Audio Engineering Society Convention 119. Audio Engineering Society.

[7] Kaizer, A. J. (1987). Modeling of the nonlinear response of an electrodynamic loudspeaker by a Volterra series expansion. Journal of the Audio Engineering Society, 35(6), 421-433.

[8] Lashkari, K. (2006, May). A novel Volterra-Wiener model for equalization of loudspeaker distortions. In Acoustics, Speech and Signal Processing, 2006. ICASSP 2006 Proceedings. 2006 IEEE International Conference on (Vol. 5, pp. V-V). IEEE.

[9] Suykens, J., Vandewalle, J., & Van Ginderdeuren, J. (1995). Feedback linearization of nonlinear distortion in electrodynamic loudspeakers. Journal of the audio engineering society, 43(9), 690-694.

[10] State-Space Modeling and Identification of Loudspeaker with Nonlinear Distortion IASTED International Conference on Modeling, Simulation, and IdentificationNovember 2011 Authors: Pascal BRUNET, Bahram Shafai

[11] Schäfer, I., & Krüger, K. (2006). Modelling of coils using fractional derivatives. Journal of Magnetism and Magnetic Materials, 307(1), 91-98.

[12] Schäfer, I., & Krüger, K. (2008). Modelling of lossy coils using fractional derivatives. Journal of Physics D: Applied Physics, 41(4), 045001.

[13] Maschke, B. M., Van der Schaft, A. J., & Breedveld, P. C. (1992). An intrinsic Hamiltonian formulation of network dynamics: Non-standard Poisson structures and gyrators. Journal of the Franklin institute, 329(5), 923-966.

[14] Van der Schaft, A. J. (2006). Port-Hamiltonian systems: an introductory survey. Proceedings of the International Congress of Mathematicians (3): Invited Lectures, 1339-1365.

[15] Stramigioli, S., Duindam, V., & Macchelli, A. (2009). Modeling and Control of Complex Physical Systems: The Port-Hamiltonian Approach. Springer.

[16] Falaize-Skrzek, A., & Hélie, T. (2013, October). Simulation of an analog circuit of a wah pedal: a port-Hamiltonian approach. In Audio Engineering Society Convention 135. Audio Engineering Society.

[17] Hélie, T., & Matignon, D. (2006). Diffusive representations for the analysis and simulation of flared acoustic pipes with visco-thermal losses. Mathematical Models and Methods in Applied Sciences, 16(04), 503-536.

[18] Le Gorrec, Y., & Matignon, D. (2012). Diffusive systems coupled to an oscillator: a Hamiltonian formulation. Lagrangian and Hamiltonian Methods for Non Linear Control., 1-6.